JOURNAL OF VIROLOGY, Aug. 2005, p. 10247–10257 Vol. 79, No. 16
0022-538X/05/$08.00+0 doi:10.1128/JVI.79.16.10247–10257.2005

Mutations That Abrogate Human Immunodeficiency Virus Type 1 Reverse Transcriptase Dimerization Affect Maturation of the Reverse Transcriptase Heterodimer

Johanna Wapling,[1,2] Katie L. Moore,[1] Secondo Sonza,[2,3] Johnson Mak,[4,5] and Gilda Tachedjian[1,2,6]*

Molecular Interactions Group, Macfarlane Burnet Institute for Medical Research and Public Health, Melbourne, Victoria 3001, Australia[1];Department of Microbiology, Monash University, Clayton, Victoria 3168, Australia[2]; HIV Regulation Laboratory, Macfarlane Burnet Institute for Medical Research and Public Heath, Melbourne, Victoria 3001, Australia[3]; HIV Assembly Group, Macfarlane Burnet Institute for Medical Research and Public Health, Melbourne, Victoria 3001, Australia[4]; Department of Biochemistry and Molecular Biology, Monash University, Clayton, Victoria 3168, Australia[5]; and Department of Medicine, Monash University, Prahran, Victoria 3181, Australia[6]

Received 8 February 2005/Accepted 16 May 2005

The specific impact of mutations that abrogate human immunodeficiency virus type 1 (HIV-1) reverse transcriptase (RT) dimerization on virus replication is not known, as mutations shown previously to inhibit RT dimerization also impact Gag-Pol stability, resulting in pleiotropic effects on HIV-1 replication. We have previously characterized mutations at codon 401 in the HIV-1 RT tryptophan repeat motif that abrogate RT dimerization in vitro, leading to a loss in polymerase activity. The introduction of the RT dimerization-inhibiting mutations W401L and W401A into HIV-1 resulted in the formation of noninfectious viruses with reduced levels of both virion-associated and intracellular RT activity compared to the wild-type virus and the W401F mutant, which does not inhibit RT dimerization in vitro. Steady-state levels of the p66 and p51 RT subunits in viral lysates of the W401L and W401A mutants were reduced, but no significant decrease in Gag-Pol was observed compared to the wild type. In contrast, there was a decrease in processing of p66 to p51 in cell lysates for the dimerization-defective mutants compared to the wild type. The treatment of transfected cells with indinavir suggested that the HIV-1 protease contributed to the degradation of virion-associated RT subunits. These data demonstrate that mutations near the RT dimer interface that abrogate RT dimerization in vitro result in the production of replication-impaired viruses without detectable effects on Gag-Pol stability or virion incorporation. The inhibition of RT activity is most likely due to a defect in RT maturation, suggesting that RT dimerization represents a valid drug target for chemotherapeutic intervention.

The human immunodeficiency virus type 1 (HIV-1) reverse transcriptase (RT) is critical for HIV-1 replication and is required for the conversion of the genomic viral RNA into a double-stranded proviral DNA precursor, catalyzed by the RNA- and DNA-dependent polymerase and RNase H activities of the enzyme. The biologically relevant form of HIV-1 RT is a heterodimer composed of 66 (p66)- and 51-kDa (p51) polypeptides. The p51 subunit is derived from and is identical to the N-terminal polymerase domain of p66 (9). The p66 subunit can be divided structurally into the polymerase and RNase H domains, with the polymerase domain further divided into the fingers, palm, thumb, and connection subdomains (24, 29). One functional polymerase and RNase H active site is located on the p66 subunit, which adopts an "open" structure to accommodate the nucleic acid template/primer (24, 29). The p51 subunit has the same polymerase subdomains as p66. However, the spatial orientations of the individual subdomains differ from those in p66, with the p51 subunit assuming a "closed" structure and playing a largely structural role in the heterodimer (2, 23, 32). Structural analyses reveal three major contacts between the p66 and p51 subunits, which include interactions between the connection subdomains of both subunits, with most of the interaction surface being largely hydrophobic (4, 59).

The appropriate association of the p66 and p51 RT subunits is required for activation of the enzyme, as monomeric subunits are devoid of polymerase activity (41, 51, 53). In vitro dimerization of the p66 and p51 subunits can be achieved under nonphysiological conditions and appears to occur by a two-step process involving the initial formation of an intermediate that can bind the template/primer but lacks polymerase activity followed by conformational changes resulting in an active enzyme (11). While this in vitro study may not exactly represent how RT maturation occurs in infected cells, it does demonstrate the absolute requirement for RT dimerization to activate polymerase function, making RT dimerization an attractive drug target (21, 48, 51, 53). Despite several in vitro studies demonstrating the critical role of RT dimerization in enzyme activation (51, 53), the specific impact of abrogating RT dimerization on HIV-1 replication has not been determined.

The HIV-1 RT is expressed as part of a Gag-Pol polyprotein ($Pr160^{gag\text{-}pol}$), which consists of the structural proteins matrix

* Corresponding author. Mailing address: Molecular Interactions Group, Macfarlane Burnet Institute for Medical Research and Public Health, 85 Commercial Road, GPO Box 2284, Melbourne, Victoria 3001, Australia. Phone: (61) 3 9282 2256. Fax: (61) 3 9282 2100. E-mail: gildat@burnet.edu.au.

(MA), capsid (CA), p2, and nucleocapsid (NC) and the Pol-encoded functional enzymes protease (PR), RT, and integrase (IN) (20). A transframe region links the Gag and the Pol domains and consists of an N-terminal octapeptide and $p6^{pol}$ that are separated by an HIV-1 protease cleavage site (15). $Pr160^{gag\text{-}pol}$ is translated from a full-length viral RNA once every 20 Gag ($Pr55^{gag}$) translation events by a ribosomal frameshift mechanism (66). Proteolytic processing by the *pol*-encoded PR results in the sequential cleavage of Gag and Gag-Pol during or shortly after viral particle release (27), resulting in the formation of mature structural proteins and viral enzymes (58). The precise pathway for the formation of RT heterodimers in HIV-1-infected cells is not established, although it is proposed to occur through a p66/p66 homodimer intermediate (59). Recent data based on a model 90-kDa Pol polyprotein (which consists of the transframe region, PR, RT, and the N terminus of IN) support this model (45). The study of mutations that abrogate RT dimerization is likely to shed light on the intermediates involved in the formation of stable RT heterodimers in HIV-1-infected cells.

The RT tryptophan repeat motif represents a remarkable cluster of six tryptophan residues, at codons 398, 401, 402, 406, 410, and 414, five of which are separated by three amino acid residues (3). The tryptophan repeat motif is found in the connection subdomain of both HIV-1 RT subunits. This hydrophobic cluster is highly conserved among primate lentiviral reverse transcriptases (3), although it is not found in other lentiviral RTs known to form heterodimers, including feline immunodeficiency virus RT. The tryptophan repeat motif is also absent from RTs from other retrovirus families, including those of the heterodimeric avian sarcoma leukosis virus and Moloney murine leukemia virus, which may dimerize when presented with a template (56). Previous studies suggested that the tryptophan repeat motif is important for RT heterodimerization, as the elucidation of the kinetics of the association of p66 and p51 RT subunits in vitro implicates the RT tryptophan residues as being involved in the initial interaction of the two monomers (10). These data are supported by our studies, which demonstrate that mutations of the highly conserved tryptophans at codons 401 and 414 in the context of the p66 subunit abrogate RT heterodimerization, as observed in both a yeast two-hybrid system for RT dimerization and in vitro binding assays (51).

The study and interpretation of the impact of mutations in RT and IN on HIV-1 replication are usually complicated by their effects on the stability and function of the Gag-Pol polyprotein from which RT and IN are expressed (34, 44, 65). A *trans*-complementation system has been developed to study the impact of mutations in specific subunits of the HIV-1 RT, where RT and IN are delivered into viral particles in *trans* fused to HIV-1 Vpr (35, 64). While this system is useful for examining the effect of RT mutations on intracellular reverse transcription, it is unlikely to recapitulate the maturation of the HIV-1 RT heterodimer from the Gag-Pol polyprotein as it occurs in HIV-1-infected cells. Hence, to examine the impact of RT dimerization-blocking mutations on RT maturation and function, it is necessary to perform these experiments in the context of the full-length virus, using mutations that are not expected to impact Gag-Pol stability or its packaging into the virion.

Examples of RT mutations at primer grip residues L234 and W229 that abrogate RT dimerization have been described (6, 14, 26, 52, 62). The primer grip region of HIV-1 RT is important for maintaining the primer terminus in an orientation appropriate for nucleophilic attack by the incoming deoxynucleoside triphosphate (37) and is not near the RT dimer interface (24, 29). Previous studies which examined the impact of mutations in or near the RT primer grip region on HIV-1 replication demonstrated decreased viral infectivity due to defects in Gag-Pol stability (65). The L234D primer grip mutant produced HIV-1 with a reduced infectivity as a result of defects in virion maturation that were ascribed to the premature cleavage of $Pr160^{gag\text{-}pol}$ in the cell, leading to a reduction in the virion incorporation of *pol* gene products (65). Since the primer grip region is far from the dimer interface, mutations at L234 that negate RT dimerization are likely to do so through long-range conformational changes that may also impact the conformation and stability of $Pr160^{gag\text{-}pol}$. In contrast, W401 is close to the RT dimer interface, and mutation of this residue to either an alanine or leucine in the context of p66 abrogates the interaction with p51 in vitro (51). Our studies demonstrate that the effect of mutating W401 is mainly localized to the repositioning of a loop region between amino acids W401 and W414 in the p66 subunit (51). Furthermore, a circular dichroism analysis of recombinant RT heterodimers expressing either the W401A or W401L mutation demonstrated no significant change in secondary structure or misfolding of the protein compared to wild-type RT (53). Since RT W401 is near the dimer interface, we hypothesized that the impact of mutations at this residue on the stability and structure of $Pr160^{gag\text{-}pol}$ would be minimal, enabling us to probe the specific effect of mutations that abrogate RT dimerization on RT maturation in the context of a full-length infectious virus.

In this study, we show that RT dimer interface mutations at amino acid W401 result in the production of viral particles with dramatically reduced infectivities and specific defects in RT maturation and function. Notably, this phenotype was observed in the absence of detectable Gag-Pol instability and virion packaging defects. Furthermore, our data provide evidence in support of the ideas that the immediate precursor of the RT heterodimer is the p66 homodimer and that the abrogation of RT dimerization represents a valid drug target for chemotherapeutic intervention.

MATERIALS AND METHODS

Cell culture. The 293T and TZM-bl (60) cell lines were maintained in Dulbecco's modified Eagle's medium (DMEM) containing 10% fetal calf serum (Progen, Darra, Queensland), glutamine (292 μg/ml), penicillin (100 U/ml), and streptomycin (100 μg/ml) (DMEM-10). TZM-bl cells were obtained through the NIH AIDS Research and Reference Reagent Program, Division of AIDS, National Institute for Allergy and Infectious Diseases (NIAID), National Institutes of Health (NIH), and were contributed by John C. Kappes, Xiaoyun Wu, and Tanzyme Inc. MT-2 cells (16) were maintained in RPMI 1640 supplemented with 10% fetal calf serum, glutamine (29.2 μg/ml), penicillin (100 U/ml), and streptomycin (100 μg/ml).

Antibodies. The monoclonal antibodies 11G10 and 5B2 recognize HIV-1 RT epitope 1 (codons 193 to 284) and HIV-1 RT epitope 2 (codons 294 to 319), respectively, and were generously provided by Dag Helland (University of Bergen, Norway) (50). The monoclonal antibody 8E5 recognizes the C-terminal epitope (codons 262 to 271) of HIV-1 IN (36) and was provided by Dag Helland. A p24 monoclonal antibody to the HIV-1 capsid (p24), purified by Andy Poumbourios (St. Vincent's Institute of Medical Research, Melbourne, Australia)

from an HIV-1 p24 hybridoma (183-H12-5C), was obtained through the NIH AIDS Research and Reference Reagent Program, Division of AIDS, NIAID, NIH, and was contributed by Bruce Chesebro (7). Pooled sera from HIV-infected patients were also used to detect HIV-1 *gag* and *pol* gene products (22).

Drug. Indinavir sulfate was prepared as a 10 mM stock in sterile water and was obtained through the NIH AIDS Research and Reference Reagent Program.

HIV-1 proviral clones and site-directed mutagenesis. The plasmid pSVC21 contains the infectious HXB2 molecular clone of HIV-1 (12). Mutations at RT amino acid W401 were introduced by site-directed mutagenesis using a Gene-Editor mutagenesis kit (Promega, Madison, Wis.) into the clone pBPol containing the Apa1-SalI fragment of HXB2 (nucleotides 2006 to 5786) cloned into the ApaI-SalI sites of pBluescript II SK(+) (Stratagene, La Jolla, CA). The mutagenic oligonucleotides 5′-GGAAACATGGGAAACCGCGTGGACAGAGTA TTGG-3′, 5′-GGAAACATGGGAAACGTTGTGGACAGAGTATTGG-3′, and 5′-GGAAACATGGGAAACATTCTGGACAGAGTATTGG-3′ were used to introduce the W401A, W401L, and W401F mutations, respectively, into the RT gene in pBPol. Following site-directed mutagenesis, the ApaI-SalI fragment in pBPol was subcloned into the ApaI-SalI sites of pSVC21 to generate the proviral mutants HX-W401A, HX-W401L, and HX-W401F. The construct pDRNL, containing the infectious NL4-3 molecular clone of HIV-1 (1), was used to generate a clone containing the W401A mutation in the RT gene (NL-W401A) by stitch PCR mutagenesis (6).

Transfections. 293T cells were seeded at 2×10^6 cells in 10-cm-diameter tissue culture plates in DMEM-10 1 day prior to transfection. Proviral DNA constructs (10 μg/plate) were introduced into cells by using the calcium phosphate procedure as previously described (38). An enhanced green fluorescent protein (EGFP; Clontech)-expressing reporter plasmid (2 μg) was cotransfected with the HIV-1 plasmids to determine the transfection efficiency. At 8 h posttransfection, cells were washed with phosphate-buffered saline without magnesium and calcium [PBS(−)] and replenished with fresh DMEM-10. At 36 h posttransfection, viruses and cells were harvested, and cell lysates were normalized according to their transfection efficiency for Western blot analysis. For the examination of viral protein profiles in viral lysates, infectivity assays, and cell-free RT assays, the amounts of virus were normalized according to equivalent amounts of virion-associated p24, as determined by Western blot analysis using p24 antibodies. For transfections performed in the presence of indinavir, cells were pretreated with 0, 0.1, 1, or 10 μM of drug, which was added to cells 1 h prior to transfection and was maintained in the culture up to the time of harvesting of cells and virus.

Infectivity assays. The titer of HIV-1 produced from 293T cell transfections was determined by end-point dilution in MT-2 cells. MT-2 cells (30,000 cells/ml) were seeded into a 96-well tissue culture plate and inoculated with 10-fold serial dilutions of virus in quintuplicate wells. Following day 6 postinfection, the virus-specific cytopathic effect was scored in each well as either positive or negative in order to calculate the 50% tissue culture infective dose using the Karber formula (18). The amount of infectious virus was determined by using the TZM-bl reporter cell line. TZM-bl cells were seeded in a 24-well tissue culture plate at 5×10^4 cells per well 1 day prior to infection. Duplicate wells were infected with a viral inoculum diluted in DMEM-10 containing DEAE-dextran (Amersham Biosciences) at a final concentration of 40 μg/ml. Cultures were incubated at 37°C in 5% CO_2 for 48 h postinfection, fixed in 0.25% glutaraldehyde-0.8% formaldehyde in PBS for 5 min at room temperature, and then stained with 400 μg/ml of X-Gal (5-bromo-4-chloro-3-indolyl-β-D-galactopyranoside), 4 mM $MgCl_2$, 4 mM potassium ferrocyanide, and 4 mM potassium ferricyanide in PBS for 1 h at 37°C. Mock-infected cells were included and used to determine the background. Following two washes with PBS, blue foci were counted by microscopy as previously described (8). The presence of equivalent amounts of virion-associated p24 in culture supernatants for mutant and wild-type strains was confirmed by a Western blot analysis of viral lysates purified through a 25% (wt/vol) sucrose cushion prior to the infectivity assays. Since the numbers of viral particles produced were similar for wild-type and mutant viruses, virus infectivity in MT-2 and TZM-bl cells was expressed per ml of culture supernatant.

Viral protein analysis. For an analysis of viral proteins by Western blotting, culture supernatants from transfected 293T cells were harvested at 36 h post-transfection and clarified by low-speed centrifugation (2,000 rpm for 30 min; Beckman GS-6R rotor), followed by concentration and partial purification of the virus through a 25% (wt/vol) sucrose cushion (26,500 rpm, 1 h, 4°C) using an SW41 rotor (Beckman). Viral pellets were solubilized in 80 μl of 2× sodium dodecyl sulfate (SDS) loading buffer and heated to 95°C for 3 min prior to the separation of proteins in a 7.5% polyacrylamide gel containing sodium dodecyl sulfate (SDS-polyacrylamide gel electrophoresis [SDS-PAGE]). For the analysis of intracellular viral protein expression, transfected 293T cells were washed twice with PBS(−), collected in 5 ml of PBS(−), and pelleted at 1,500 rpm for 10 min. The cell pellet was lysed in 500 μl of TNEN (10 mM Tris, pH 8.0, 50 mM NaCl, 1 mM EDTA, 1.0% Igepal CA-630 [Sigma-Aldrich, Castle Hill, NSW, Australia]) containing 1 μg/ml each of aprotinin, leupeptin, and pepstatin. For experiments performed with indinavir, the lysis buffer was also supplemented with 10 μM drug. Lysates were centrifuged at 13,000 × *g* at 4°C for 20 min, and the supernatants were removed, added to an equal volume of 2× SDS loading buffer, heated to 95°C for 3 min, and then subjected to SDS-PAGE. Following electrophoresis, proteins were transferred to polyvinylidene difluoride membranes (Millipore, North Ryde, NSW, Australia) by electroblotting and blocked for 1 h at room temperature with 5% skim milk power in TBST (0.5% Tween 20, 137 mM NaCl, 20 mM Tris), followed by incubation with primary and secondary antibodies conjugated to horseradish peroxidase (Amersham Biosciences). Viral proteins were detected by chemiluminescence per the manufacturer's instructions (Amersham Biosciences). The quantitation of viral protein bands from Western blots was performed by densitometry using ScienceLab 99 Image Gauge, version 3.3, software (Fuji Photo Film Co. Ltd.) as previously described (28). The statistical significance of differences between mutant and wild-type proteins was determined using the Wilcoxon rank sum test (5, 42) for a minimum of three independent assays, with data expressed as average relative intensities ± standard deviations. The relative viral release efficiency (viral production) was calculated as the amount of viral particle-associated Gag divided by the total (cell- and viral particle-associated) amount of Gag as described previously (43).

Cell-free reverse transcriptase assay. Clarified viral lysates from transfections were applied to an equal volume of 0.3% Igepal CA-630. The RT activity of viral lysates (20 μl) was assayed in the presence of 5 μg/ml poly(rA)/oligo(dT) (Amersham Biosciences), 10 μCi [α-^{33}P]dTTP (Perkin-Elmer, Boston, MA), 50 mM Tris, pH 7.8, 7.5 mM KCl, 2 mM dithiothreitol, and 5 mM $MgCl_2$ for 2 h at 37°C. Samples were applied to DE 81 membranes and washed, and incorporated counts were quantified by phosphorimager analysis as previously described (52).

Intracellular reverse transcriptase assay. Semiquantitative PCR was used to detect reverse transcripts in lysates of MT-2 cells (4×10^5 cells/10 ml) infected with wild-type and mutant viruses (500 ng of p24 quantified using the Vironostika HIV-1 Antigen MicroElisa system [Biomerieux, Baulkham Hills, NSW, Australia]) which were harvested at 6 h postinfection. Cells were washed with PBS(−) and prepared for PCR as previously described (49), except that cells were lysed with 100 μl of lysis buffer (1× HotStarTaq PCR buffer [QIAGEN, Clifton Hill, Victoria, Australia], 0.5% Igepal CA-630, 0.5% Tween 20). Prior to infection, viral stocks were filtered through 0.45-μm filters and pretreated with 10 U of RNase-free DNase I (Roche, Castle Hill, NSW, Australia) for 30 min at 37°C in the presence of 10 mM $MgCl_2$ to remove contaminating plasmid DNA. Ten-microliter aliquots of undiluted cell lysates and either a 1/3, 1/10, or 1/30 dilution of the cell lysates were assayed by PCR using HotStarTaq DNA polymerase (QIAGEN) in a 50-μl reaction mixture to detect early viral DNA synthesis (R/U5) using the primer pair M667 (5′-GGCTAACTAGGGAACCCACTG-3′) and AA55 (5′-CTGCTAGAGATTTTCCACACTGAC-3′) (66). The presence of full-length or nearly full-length (long terminal repeat [LTR]/*gag*) viral DNA transcripts was detected by PCR using the primer pair M667 and M661 (5′-CC TGCGTCGAGAGAGCTCCTCTGG-3′) (66).

The amount of DNA in the lysates was standardized by PCR using the HLA-DQα-specific primers GH26 (5′-GTGCTGCAGGTGTAAACTTGTACCAG-3′) and GH27 (5′-CACGGATCCGGTAGCAGCGGTAGAGTTG-3′ (30). Lysates from ACH2 cells, which contain a single copy of proviral DNA per cell (13), were used for PCR quantitation as previously described (49).

Protein purification and size exclusion chromatography. Recombinant p66-His and p66W401A-His were purified by Ni-nitrilotriacetic acid and DEAE-Sepharose chromatography as previously described (31). The separation of RT monomers and homodimers was performed by size exclusion chromatography (SEC) using a Superdex 200 column (Amersham Biosciences) and a Pharmacia fast-performance liquid chromatography system. The elution of RT subunits was compared to the elution profiles of a mixture of eight molecular size standards for gel filtration (range, 669 to 13.7 kDa) per the manufacturer's instructions (Amersham Biosciences). Samples (200 μl) were resolved using a mobile-phase (50 mM sodium phosphate, pH 7.8, 150 mM NaCl) flow rate of 0.25 ml/min. To examine the proportions of monomers versus homodimers, purified wild-type p66 or mutant p66W401A-His was diluted in the mobile phase to a final concentration of 3.8 μM and resolved by SEC after 2 h of incubation on ice.

RESULTS

Mutations at RT codon 401 do not affect viral particle production and Gag processing in virions. We have previously demonstrated that the RT mutations W401A and W401L negate RT dimerization both in vitro and in the yeast two-hybrid

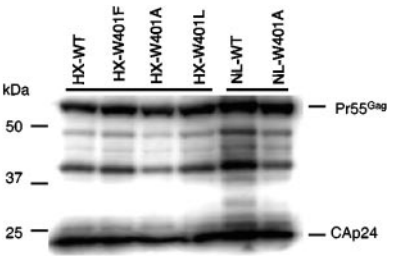

FIG. 1. Viral lysates probed with p24 antibodies. 293T cells were cotransfected with an EGFP reporter plasmid and infectious molecular clones of wild-type HIV-1 (HX-WT and NL-WT) or the W401 RT mutants HX-W401F, HX-W401A, HX-W401L, and NL-W401A. At 36 h posttransfection, viruses and cells were harvested and normalized to the transfection efficiency (according to EGFP expression) and virion-associated p24 by Western blot analysis for the elucidation of viral protein profiles in viral and cell lysates. Viruses were purified from cell culture supernatants at 36 h posttransfection by centrifugation through a 25% (wt/vol) sucrose cushion. Viral pellets were solubilized in 2× SDS loading buffer, and proteins were separated by SDS-PAGE on a 7.5% polyacrylamide gel and subjected to Western blot analysis using p24 antibodies. Viral bands were visualized by chemiluminescence.

system, while W401F has no effect on RT dimerization (51). To determine if mutations that abrogate RT dimerization affect viral production, we transfected 293T cells with infectious molecular clones of HIV-1 expressing the W401A (HX-W401A and NL-W401A), W401L (HX-W401L), and W401F (HX-W401F) RT mutations and compared the viral protein profiles of the mutants to those of the corresponding isogenic wild-type strains (HX-WT or NL-WT) (51) in both viral and cell lysates. We examined the effect of the W401A mutation in the HXB-2 and NL4-3 genetic backgrounds to ensure that any observed phenotypic effects were not strain dependent.

A Western blot analysis of both viral (Fig. 1) and cell lysates (data not shown) from HIV-transfected cells probed with p24 antibodies demonstrated similar expression levels of viral Gag for the mutant and isogenic wild-type strains. The relative viral release efficiencies ± standard errors for the mutant viruses normalized to that of the wild type were 101 ± 12 for HX-W401F, 100 ± 14 for HX-W401A, 98 ± 13 for HX-W401L, and 109 ± 17 for NL-W401A. Statistical analysis demonstrated that viral production was not significantly different for the mutant W401 viruses compared to the isogenic wild-type strains. These data demonstrate that mutations at W401 do not affect viral particle production.

To determine whether the processing of $Pr55^{gag}$ to p24 was altered in the mutant viruses, we performed a Western blot analysis of viral lysates probed with p24 antibodies and determined the ratio of p24 to $Pr55^{gag}$ for HX-W401A, HX-W401L, and HX-W401F compared to that for the wild-type virus (Fig. 1). Our analysis revealed no significant difference in the p24/$Pr55^{gag}$ ratio for the mutants compared to that for the wild-type virus (HX-WT, 1.10 ± 0.05; HX-W401F, 1.05 ± 0.11; HX-W401A, 1.07 ± 0.04; HX-W401L, 1.04 ± 0.06). A similar investigation of HIV-1 containing the W401A mutation in the NL4-3 genetic backbone (NL-W401A) also revealed no significant difference in the processing pattern of $Pr55^{gag}$ to p24 compared to that for NL-WT (NL-WT, 1.05 ± 0.04; NL-W401A, 1.04 ± 0.05) (Fig. 1). Taken together, these data demonstrate that mutations near the RT dimer interface that abrogate RT dimerization result in viruses that produce normal levels of viral particles with no detectable defects in Gag processing.

The W401A/L RT mutations result in viral particles with reduced infectivities. Since RT dimerization is critical for activation of the RT enzyme (51, 53), we hypothesized that mutations that cause defects in RT subunit interactions would have detrimental effects on viral infectivity. In order to determine whether the viral particles with mutations at RT W401 were infectious, we subjected viruses obtained from the transfection of 293T cells with the HIV-1 wild type and with mutant clones to infectivity assays performed in MT-2 and TZM-bl cells. For the detection of virus replication in MT-2 cells, the virus must undergo multiple rounds of replication and spread through the culture to produce detectable virus-specific cytopathic effects by 6 days postinfection. Consequently, any differences in viral infectivity will be amplified in this system compared to assays in which the virus undergoes limited rounds of infection, such as assays with the TZM-bl cell line. The HIV-1 mutants HX-W401A, HX-W401L, and NL-W401A demonstrated undetectable levels of infectious virus in MT-2 cells, while the titer of HX-W401F was fourfold less than that of the wild type (Fig. 2A). We also assessed the infectivity of the mutant viruses in the TZM-bl indicator cell line, which contains a host cell chromosome-integrated LacZ gene under the control of the HIV-1 LTR promoter (8). These cells can measure a single round of infection, which is detected by transactivation of the LacZ reporter by newly synthesized Tat protein following integration of the viral DNA. Therefore, HIV-1 with defects in the early stage of replication up to and including integration and the production of Tat would be expected to display a reduced infectivity in this cell line. Under our assay conditions (48 h), the cells would have been subjected to limited rounds of HIV infection. In this assay, HX-W401L was noninfectious while HX-W401F was 2.5-fold less infectious than HX-WT (Fig. 2B), similar to the data we observed with the MT-2 infectivity assay. In contrast to the results of the infectivity assay performed with MT-2 cells, the HX-W401A and NL-W401A mutants demonstrated the presence of infectious virus. Nevertheless, their infectivities were significantly lower than that of the corresponding wild-type strains, with 100- and 50-fold decreases for HX-W401A and NL-W401A, respectively (Fig. 2B). These data demonstrate a correlation between the abrogation of RT dimerization in vitro and defects in viral infectivity.

The W401A/L RT mutations result in viral particles with defects in both virion particle-associated and intracellular RT activity. We have shown that the HIV-1 mutants displayed significant defects in infectivity (Fig. 2). We also know from previous studies that viruses with mutations at W401 that abrogate RT dimerization in vitro lack RT activity (51, 53). Therefore, we examined the RT activity present in viral particles and the capacity of the RT in these particles to initiate and complete intracellular reverse transcription. To measure RT activity in virions, viral particles from 293T transfections (normalized for p24) were subjected to a cell-free RT assay using poly(rA)/oligo(dT) as a template primer. HX-W401A, HX-W401L, and NL-W401A displayed <1% of the RT activity of the wild type in our assay, while the RT activity of the HX-

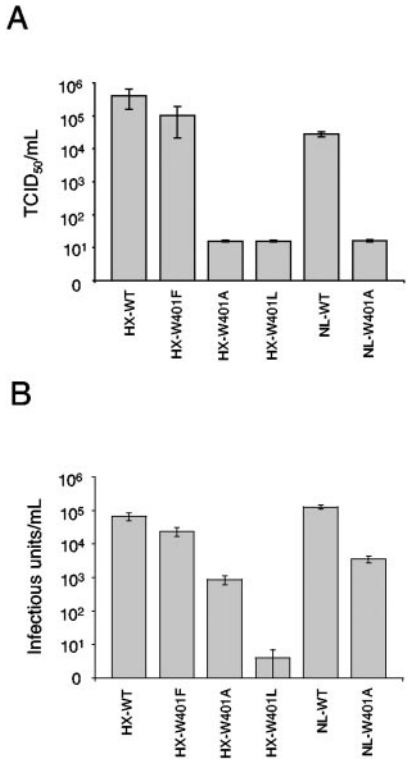

FIG. 2. Infectivities of wild-type and W401 mutant viruses produced by transfection of 293T cells. Prior to infection, clarified 293T cell supernatants containing wild-type or mutant virus were normalized to equivalent amounts of virion-associated p24, as determined by Western blot analysis. (A) Infectivities determined in a 6-day spreading assay performed with MT-2 cells. Cells were infected in quintuplicate wells with 10-fold serial dilutions of virus. At 6 days postinfection, the virus-specific cytopathic effect was scored and the 50% tissue culture infective dose ($TCID_{50}$) was calculated for each virus. Results were obtained from three independent assays. (B) Infectivities determined with TZM-bl cells. Serially diluted viruses were used to infect duplicate wells, and the numbers of blue-staining foci (infectious units) were determined at 48 h postinfection as described in Materials and Methods. Data were obtained from two independent assays. Error bars indicate standard deviations.

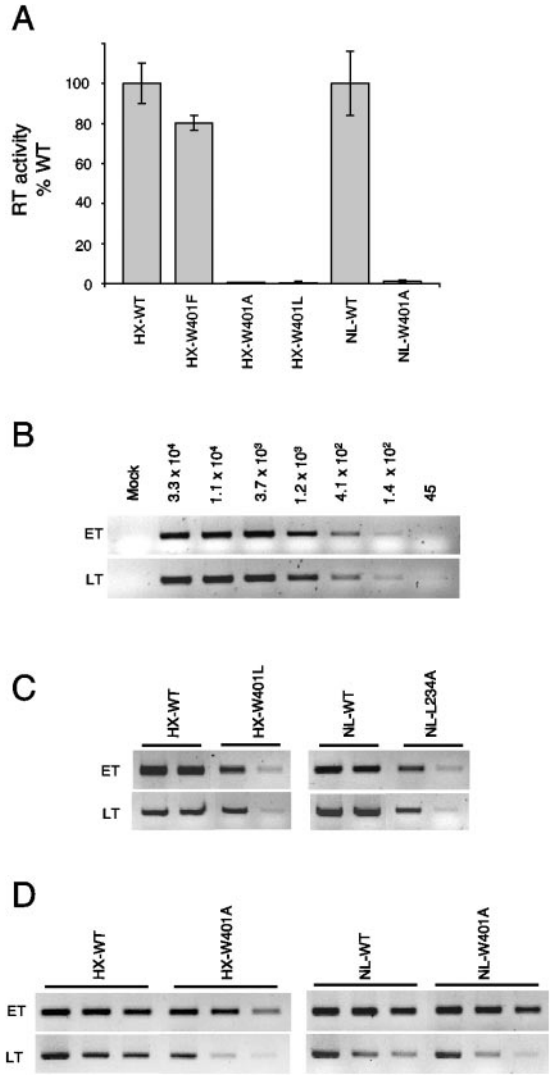

FIG. 3. RT activities of wild-type and W401 mutant viruses. (A) Viruses from cell culture supernatants obtained from transfected 293T cells expressing wild-type and W401 mutant viruses were normalized to equivalent amounts of virion-associated p24, as determined by Western blotting, lysed, and subjected to a cell-free RT assay using a poly(rA)/oligo(dT) template/primer and an [α-^{33}P]dTTP substrate. Incorporated counts were determined by phosphorimager analysis. Results were obtained from three independent assays. Error bars indicate standard deviations. (B, C, and D) Semiquantitative PCRs for viral DNA transcripts. The primer pair AA55 and MM67 was used to detect early transcripts (ET), and MM61 and MM67 were used to detect late transcripts (LT). (B) Dilution series of ACH2 cell lysate, which contains one integrated copy of the HIV-1 provirus per cell, in addition to PCR of uninfected MT-2 cells (mock). For panels C and D, supernatants from transfected 293T cells were clarified, treated with DNase I, and used to infect MT2 cells using 500 ng of p24/4 $\times$ 10^5 cells. At 6 hours postinfection, the cells were collected, lysed, and then subjected to PCR analysis. (C) PCRs were performed on undiluted (left) and diluted (1/10) (right) MT-2 cell lysates infected with HX-W401L, NL-L234A, and corresponding wild-type viruses. (D) MT-2 cell lysates from infections with HX-W401A, NL-W401A, and corresponding wild-type viruses were diluted 1/3, 1/10, and 1/30 (left to right). PCR products were resolved in a 2% agarose gel and visualized by ethidium bromide staining. The absence of contaminating plasmid DNA was confirmed by performing PCR on the DNase I-treated cell culture supernatant used for MT2 infection using both primer pairs (data not shown).

W401F virus was 80% that of the wild type (Fig. 3A). These data clearly show that viruses containing mutations known to abrogate RT dimerization in vitro are defective in RT function.

To determine whether viral particles could initiate and complete intracellular reverse transcription, we performed a semiquantitative PCR using primers that detect early transcripts (minus-strand strong-stop DNA) and primers designed to detect nearly complete viral DNA transcripts (66). MT-2 cells were infected with viruses (normalized for p24) and at 6 h postinfection were lysed for PCR analysis. A housekeeping gene, HLA-DQα, was amplified from cell lysates and used to normalize the cell lysates subjected to PCR for the detection of HIV-1 reverse transcripts (data not shown).

HX401L demonstrated dramatic decreases in both early and late transcripts (Fig. 3C). We also tested HIV-1 expressing the L234A RT mutation (NL-L234A). Mutations at this residue have been reported to confer a defect in Gag-Pol packaging, and as a result, decreased packaging of RT in the virion (6, 65). Hence, the NL-L234A mutant was expected to demonstrate a

significant defect in intracellular RT function, as described for the L234D mutant (65). In our system, NL-L234A was defective in the synthesis of both early and late transcripts compared to the isogenic wild-type strain (Fig. 3B).

An analysis of the early and late transcripts synthesized by the HX-W401A and NL-W401A mutants demonstrated detectable decreases in both early and late transcripts compared to HX-WT and NL-WT, respectively (Fig. 3D). The defects in intracellular reverse transcription observed for the W401A mutants were not as dramatic as those observed for the HX-W401L mutant, particularly for early transcripts. These data are consistent with the infectivity results obtained for these mutants in the TZM-bl assay (Fig. 2B) and suggest that the decrease in infectivity in these cells can be ascribed to a defect in intracellular reverse transcription by the mutant RT enzymes.

The W401A/L RT mutations result in decreased levels of RT in virions despite normal levels of Gag-Pol incorporation. Our data suggest that mutations at the dimer interface that abrogate RT dimerization in vitro result in the production of viral particles with markedly reduced infectivity as a result of defects in RT function. One possibility for the RT defect is a reduced incorporation of Gag-Pol in the virion, as described previously (65). To exclude this possibility, we subjected viral lysates to Western blot analysis with anti-RT (11G10) and anti-IN (8E5) monoclonal antibodies (Fig. 4A). Compared to the wild type and HX-W401F, both the HX-W401A and HX-W401L mutants displayed reduced steady-state levels of the p66 and p51 RT subunits (ratio of viral p66wt to p66 mutant HX-W401F, 1.09 ± 0.37 [$P > 0.125$]; ratio of p66wt to HX-W401A, 0.59 ± 0.14 [$P = 0.048$]; ratio of p66wt to HX-W401L, 0.39 ± 0.16 [$P = 0.048$]; ratio of viral p51wt to p51 mutant HX-W401F, 1.06 ± 0.23 [$P > 0.125$]; ratio of p51wt to HX-W401A, 0.57 ± 0.16 [$P = 0.028$]; ratio of p51wt to HX-W401L, 0.35 ± 0.10 [$P = 0.008$]).

An analysis of the NL-W401A mutant also demonstrated a trend toward lower levels of p66 and p51 in the virion than those for NL-WT, which did not reach statistical significance for p51 (ratio of viral p66wt to p66 mutant NL-W401A, 0.62 ± 0.10 [$P = 0.048$]; ratio of viral p51wt to p51 mutant NL-W401A, 0.78 ± 0.11 [$P = 0.11$]). Decreased levels of the two RT subunits were also observed in viral lysates probed with another RT monoclonal antibody (5B2) and with pooled sera from HIV-infected individuals, indicating that the observed results were not RT antibody specific (data not shown).

In contrast, no significant decrease in steady-state protein levels of either Gag-Pol (the ratio of viral Gag-Pol to p24 for HX-W401F normalized to the wild type was 1.04 ± 0.18, that for HX-W401A was 0.96 ± 0.08, that for HX-W401L was 0.89 ± 0.19, and that for NL-W401A was 1.17 ± 0.24) or IN (the ratio of viral IN to p24 for HX-W401F normalized to the wild type was 1.1 ± 0.05, that for HX-W401A was 0.92 ± 0.14, that for HX-W401L was 1.01 ± 0.19, and that for NL-W401A was 1.01 ± 0.01) was detected in mutant virions compared to the corresponding wild-type virus, suggesting that the decreased levels of RT were unlikely to be a result of a defect in Gag-Pol incorporation (Fig. 4A). These data are also consistent with the lack of Gag processing defects observed in virions (Fig. 1) and indicate that normal levels of PR and therefore of Gag-Pol were incorporated into the mutant virus.

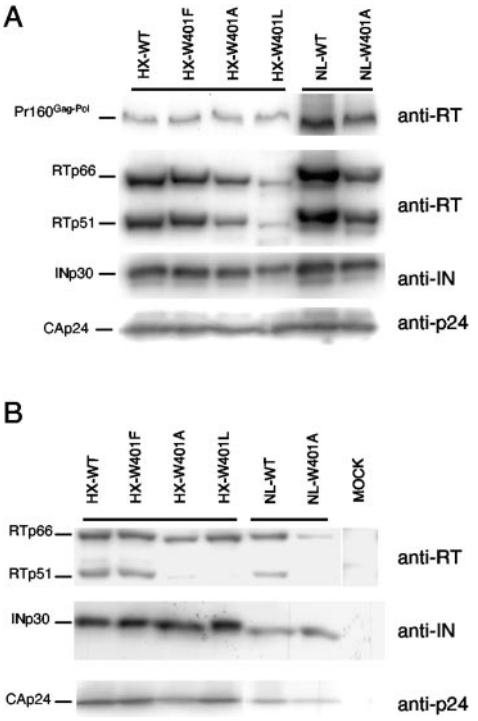

FIG. 4. HIV protein profiles of viral and cell lysates from wild-type and W401 mutant viruses. Viruses produced from 293T cells transfected with infectious molecular clones of HIV-1 expressing wild-type virus and the W401 RT mutants were purified through a 25% (wt/vol) sucrose cushion, and viral pellets were solubilized in 2× SDS loading buffer. 293T cells were washed, lysed, and clarified by centrifugation, and equal volumes were added to 2× SDS loading buffer. Viral (A) and cell (B) lysates were normalized according to virion-associated p24 (by Western blotting) and transfection efficiency, separated by SDS-PAGE on a 7.5% polyacrylamide gel, subjected to Western blot analysis using RT (11G10) and IN (8E5) antibodies, and visualized by chemiluminescence.

Intracellular processing of RT suggests a defect in p66 homodimer formation. It has been postulated that the immediate precursor to the HIV-1 RT heterodimer is the p66 homodimer (59). Since both p66 subunits contain an RNase H domain, it has been proposed that the RNase H domain of one of the subunits must unravel in the p66 homodimer, exposing the PR cleavage site between the Pol and RNase H domains and leading to a 1:1 ratio of p66 to p51 in the virion (59). In vitro studies using a minimal *pol* construct expressed in bacteria support this hypothesis (45), but there are no data to shed light on the mechanism of RT heterodimer formation in HIV-1-infected cells. We have demonstrated that the W401A RT mutation can abrogate RT heterodimerization (51) and p66 homodimerization (data not shown) in vitro. Hence, if the p66 homodimer is the immediate precursor to the RT heterodimer, then the abrogation of p66 homodimerization should lead to a decrease in processing to p51.

In order to gain insight into the nature of the immediate RT heterodimer precursor, we examined RT expression in cell lysates (Fig. 4B) of cells transfected with mutant and wild-type viruses. Cell lysates from cells transfected with the virus expressing the W401A or W401L mutant displayed altered RT processing profiles, where p51 was almost undetectable despite

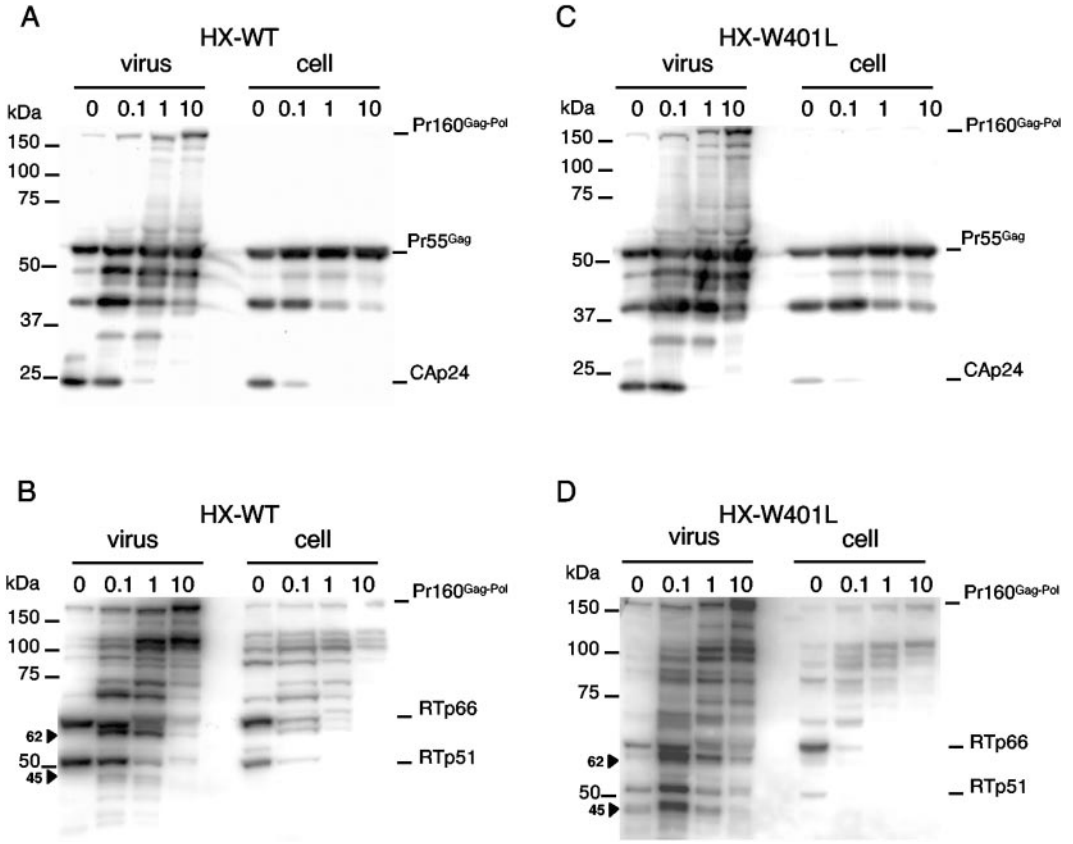

FIG. 5. Western blot analysis of wild-type and W401L mutant viruses generated in the presence of the HIV-1 protease inhibitor indinavir. 293T cells cultured in the presence of 0, 0.1, 1, or 10 μM indinavir were transfected with HX-WT and HX-W401L constructs. Cell and viral lysates were collected as described in Materials and Methods, normalized according to transfection efficiency, and subjected to SDS-PAGE and Western blot analysis. Viral and cell lysates were probed with a p24 antibody (HX-WT [A] and HX-W401L [C]) or the RT antibody 11G10 (HX-WT [B] and HX-W401L [D]). RT-related bands migrating at 62 and 45 kDa are denoted by solid arrowheads.

the presence of p66, compared with those from wild type-transfected cells and cells transfected with the dimerization-competent HX-W401F mutant (ratios of intracellular p66 to p51 for wild-type and mutant viruses were as follows: HX-WT, 1.97 ± 0.31; HX-W401F, 1.66 ± 0.42 [$P = 0.190$]; HX-W401A, 3.44 ± 0.94 [$P = 0.008$]; HX-W401L, 5.40 ± 2.17 [$P = 0.008$]; NL-WT, 1.98 ± 0.39; NL-W401A, 3.20 ± 0.48 [$P = 0.05$]). In contrast, there was no detectable change in the intracellular level of IN, suggesting that the defect was specific to RT processing (Fig. 4B). The defect in processing to p51 can be explained by the inability of p66 to form homodimers, which may be a prerequisite for heterodimer formation. Taken together, these data suggest that mutations near the dimer interface which negate RT dimerization in vitro lead to a defect in the processing of p66 to the p51 subunit inside the infected cell.

Mutant RT subunits are sensitive to proteolysis by HIV-1 protease. The decreased levels of RT in viral particles observed with the HX-W401A/L and NL-W401A mutants is likely a result of an increased susceptibility of the RT to proteolytic degradation by proteases and not of decreased expression or incorporation of Gag-Pol into the virion. To determine whether the RT subunits were degraded by HIV-1 protease, we transfected 293T cells with HX-WT and HX-W401L in the absence and presence of indinavir, a specific inhibitor of HIV-1 protease (57), and probed viral and cell lysates with either anti-p24 or the RT antibody 11G10. As expected, indinavir treatment resulted in a dose-dependent inhibition of $Pr55^{gag}$ processing to p24 for both wild-type (Fig. 5A) and mutant viruses (Fig. 5C). As shown in Fig. 4A, viral lysates from HX-WT obtained from transfections performed in the absence of indinavir demonstrated almost a 1:1 ratio of p66:p51 in the virion, and both subunits were also detectable in the cell lysates (Fig. 5B). In contrast, markedly reduced steady-state protein levels of p66 and p51 were observed in the HX-W401L viral lysates in the absence of indinavir, while in cell lysates there were decreased levels of p51 compared to HX-WT cell lysates (Fig. 5B and D). The treatment of cells transfected with HX-WT with increasing concentrations of indinavir led to a dose-dependent decrease in the processing of Gag-Pol to p66 and p51 in both viral and cell lysates (Fig. 5B). Notably, viral lysates from cells transfected with HX-W401L and treated with 0.1 μM indinavir demonstrated levels of p66 and p51 approaching those observed with the wild-type virus cultured in the absence of the drug. These data indicate that mutant RT is more susceptible to proteolytic degradation than wild-type RT and that HIV-1 PR is largely responsible for the reduced levels of RT observed in HX-W401L virions.

Restored levels of virion RT in HX-W401L treated with indinavir are not associated with restored RT activity. We observed steady-state protein levels of p66 and p51 in viral lysates from cells transfected with HX401L in the presence of 0.1 μM indinavir which approached the levels observed with the untreated wild-type virus (Fig. 5B and D). To determine whether the RT in HX-W401L virions was functional, we subjected virions to a cell-free RT assay. Virions obtained from cells transfected with HX-WT in the absence of drug displayed the highest RT activity, while decreased RT activity was observed in virions from cells treated with increasing concentrations of indinavir (data not shown). These data correlate with a decrease in the processing of Gag-Pol to p66 and p51 in the virion with increasing concentrations of indinavir (Fig. 5B). In contrast, RT from cells transfected with HX-W401L was devoid of RT activity when cultured in the absence and presence of indinavir (data not shown), despite the increased levels of p66 and p51 observed in the presence of 0.1 μM indinavir (Fig. 5D). Our data demonstrate that the p66 and p51 RT subunits in HX-W401L do not form a functional RT enzyme, despite increased expression levels of these subunits in the presence of 0.1 μM indinavir. These data suggest that the RT subunits fail to form a stable heterodimer, which is consistent with our previously described in vitro findings with recombinant RT expressing this mutation (51).

The W401A mutation abrogates p66 homodimerization in vitro. Our previous studies demonstrated that mutations that abrogate RT dimerization (W401A/L) result in a recombinant RT that fails to form a stable p66/p51 heterodimer. Furthermore, this dimerization-defective RT is devoid of RT activity, as measured in an assay using an exogenous template/primer (51). If the p66 homodimer is the immediate precursor of the RT heterodimer, it is important to establish that mutations that abrogate RT heterodimerization will also abrogate p66 homodimerization. Accordingly, we introduced the W401A mutation into a construct expressing p66 with a C-terminal histidine tag, expressed the mutant (p66W401A-His) in bacteria, and purified the protein using nickel-nitrilotriacetic acid and ion-exchange chromatography. Wild-type p66-His was also expressed and purified in the same way. The proportion of homodimer to monomer was resolved by SEC analysis on a Superdex 200 column. Wild-type His-p66 at a concentration of 3.8 μM was resolved as two peaks, representing p66 homodimers (132 kDa) and p66 monomers (data not shown), consistent with the known dissociation constant (K_D) for p66 homodimerization (59). In contrast, p66W401A at the same concentration was predominately monomeric (data not shown). These data demonstrate that mutations that abrogate RT heterodimerization also lead to defects in p66 homodimerization.

DISCUSSION

We used mutations near the RT dimer interface which were previously shown to inhibit RT heterodimerization in vitro to probe the specific effects of abrogating RT dimerization on HIV-1 replication. Our data show that the RT mutations W401A and W401L result in the production of viruses with markedly reduced infectivities due to decreased RT activity, as observed both in cell-free RT assays and at the level of intracellular reverse transcription. Furthermore, decreases in the steady-state levels of the p66 and p51 RT subunits for the W401L and W401A mutants were observed in virion lysates. Importantly, the W401F mutation, shown not to significantly inhibit RT dimerization in vitro, resulted in virions with relatively small defects in viral infectivity, RT activity, and RT maturation. These data indicate a strong correlation between the abrogation of RT dimerization and defects in RT function and maturation. Notably, the defect in viral infectivity was remarkably specific to RT and did not appear to be a result of the W401A/L mutations altering either Gag-Pol stability or the incorporation of Gag-Pol into the virions.

The observed reductions in both RT activity and steady-state protein levels of virion-associated p66 and p51 for the W401A and W401L mutants can be ascribed to three possible mechanisms: (i) an inability of the RT subunits to form stable and functional dimers, thereby inhibiting RT function; (ii) an increased susceptibility of the RT subunits to proteolytic degradation by HIV-1 PR; and (iii) an increased susceptibility of a Gag-Pol processing intermediate expressing RT to proteolytic degradation by HIV-1 PR. Consistent with the first mechanism is our observation that despite the restoration of p66 and p51 in HX-W401L virions to levels approaching those of the wild type by indinavir treatment, the RT was nonfunctional in a cell-free RT assay. The inability to form stable RT heterodimers and homodimers may also account for the increased susceptibility of mutant RT to proteolytic degradation by HIV-1 PR and possibly cellular proteases. We believe that the third possibility is unlikely, as we did not observe a concomitant degradation of HIV-1 IN along with the RT subunits in either viral or cell lysates.

HIV PR-mediated processing of Gag and Gag-Pol is critical for virus maturation (58). Gag processing occurs in a highly ordered and sequential manner which is crucial for the production of infectious virus (61). The processing of Gag-Pol is also likely to occur in a highly regulated and sequential manner for virion incorporation and proper maturation of the HIV-1 enzymes. The nature of the Gag-Pol cleavage intermediates in HIV-1-infected cells has been determined by immunoblotting using distinct antisera against HIV-1 proteins (33). The intermediates include the initial autocatalytic cleavage reaction products p120 and p113 (33). These products have also been observed with a cell-free rabbit reticulocyte lysate system for the study of PR activation in the context of full-length Gag-Pol and are generated by autocatalytic cleavage between p2/NC and transframe protein/$p6^{pol}$ (39, 40). Other processing intermediates identified in HIV-1-infected cells include PR-RT-IN (p107) and RT-IN (p97) (33). While the Gag-Pol processing intermediates have been identified, we still do not know the sequence of appearance of the processing products, which would shed light on the Gag-Pol processing precursors that are critical for RT maturation.

Two models have been proposed for the formation of the p66/p51 RT during HIV-1 PR-mediated processing of $Pr160^{gag\text{-}pol}$ (45). In the so-called sequential model, the RT heterodimer is formed from a p66/p66 homodimer intermediate, while in the concerted model, the p66 subunits are formed by processing from separate Gag-Pol molecules followed by cleavage of some of the p66 to p51, which then associates with the remaining p66. Structural studies (59) and experiments

using a model Pol polyprotein (45) support the sequential model, but no data exist to support this model in HIV-1-infected cells. Our data demonstrate that the intracellular processing of p66 to p51 in dimerization-defective mutants is not efficient and that recombinant p66W401A does not form stable p66/p66 homodimers in vitro. These data suggest that the reduced processing of p66 to p51 in cell lysates may be explained by a failure of the mutant p66 to form homodimers. An alternative explanation for the reduced intracellular processing of p66 to p51 is that the W401A/L mutations alter the conformation of p66 in such a way that the PR cleavage site between the polymerase and the RNase H domain is not accessible. However, this possibility is not consistent with our observation of a processing profile for the virion where the ratio of p66 to p51 was similar to that of the wild type. Furthermore, a circular dichroism analysis of recombinant RT mutants expressing either the W401A or W401L mutation demonstrated identical profiles to that of wild-type RT, indicating that these mutations do not lead to major changes in the RT secondary structure (53). Therefore, our data support the sequential model for p66/p51 heterodimer formation, as observed in cell lysates.

Paradoxically, while the processing of p66 to p51 was not efficient in cells transfected with HX-W401A, HX-W401L, and NL-W401A, the processing of p66 to p51 was not dramatically inhibited in the viral particles, although the steady-state levels of both subunits were less than those in the wild-type virus for the HX-W401L and HX-W401A mutants. Since the effective concentration of p66 subunits would be much higher in the confines of the viral particle than in the cell, a possible explanation for the difference in the RT processing pattern in cells compared to virions is that mutant p66 is able to form loose or transient homodimers in the virus, allowing cleavage of the RNase H domain from one of the p66 monomers to p51. Furthermore, the relative inability to form stable dimers may explain the decreased stability of the RT subunits in response to the high concentrations of HIV-1 PR in the virion, as monomeric or loose dimers of RT may be more susceptible to proteolysis than stable RT dimers. Our hypothesis of weak/transient dimer formation is consistent with the defects in RT activity observed for the dimerization-defective mutants, since it has been established that not only abrogation of RT dimerization but also destabilization of the RT dimer leads to defects in polymerase function (48). This has been demonstrated by studies with the nonnucleoside reverse transcriptase inhibitors 1-{spiro[4-amino-2,2-dioxo-1,2-oxathiole-5,3′-[2′,5′-bis-*O*-(*tert*-butyldimethylsilyl)-β-D-ribofuranosyl]]}-3-ethylthymine (TSAOe^{3}T) and (4-*tert*-butylbenzoyl)-2-hydroxy-1-naphthaldehyde hydrazone (BBSH), which both inhibit the HIV-1 RT DNA polymerase activity of the heterodimers and p66 homodimers by destabilization and not by abrogation of the RT subunit interaction (46, 47). The treatment of recombinant wild-type p66 and the W401A mutant RT with HIV-1 protease will help to determine the relative susceptibilities of monomeric and dimeric forms to proteolytic degradation in addition to whether the cleavage site between Pol and RNase H is accessible in the W401A mutant monomer.

Treatment with 0.1 μM indinavir resulted in a partial restoration of the steady-state levels of p66 and p51 in the HX-W401L mutant viral particles, but RT activity remained undetectable. We believe that the lack of RT activity in the cell-free RT assay was due to the inability of the p66 and p51 RT subunits to form stable heterodimers, as demonstrated in our previous in vitro studies (51, 53). The lack of activity is unlikely to be due to an inhibition of RT activity by the 62-kDa polypeptide (migrating immediately underneath RT p66 in Fig. 5D) recognized by the RT antibody. A peptide of this size was also observed for the wild-type virus treated with 0.1 μM indinavir (Fig. 5B), which, in contrast to the W401L mutant, displayed significant levels of RT activity (50%) compared to untreated wild-type virus (data not shown). An RT-specific band at 45 kDa was also observed in HX-W401L viral lysates harvested from 0.1 μM indinavir-treated cells. In other experiments, this band had similar intensities for both HX-WT and HX-W401L treated with 0.1 μM indinavir, indicating that it is unlikely to be specific to the HX-W401L mutant. Furthermore, the 45-kDa band is unlikely to interfere with heterodimer formation, as a deletion of as little as 26 amino acids from p51 negates the interaction with p66 (25, 52).

The W401A and W401L mutant RTs displayed a >99% reduction in RNA-dependent DNA polymerase activity compared to wild-type RT in the cell-free RT assay. A significant reduction was also observed for minus-strand strong-stop and late DNA synthesis for the W401L mutant and the L234A control compared to wild-type HIV-1. In contrast, while the virion-associated reverse transcriptase activity was dramatically reduced compared to that of the wild type, we could still detect significant levels of early DNA synthesis for NL-W401A and HX-W401A compared to the wild type, with reverse transcription defects becoming more apparent when we examined late DNA transcripts. The greater RT defect by the W401L mutation than by the W401A mutation correlates with the larger decrease in viral infectivity of HX-W401L than of HX-W401A in the infectivity assay performed with the TZM-bl cell line. One possible explanation for detectable intracellular reverse transcription, particularly for the W401A mutants, is that the RT may behave differently on an artificial template/primer from how it behaves when presented with the natural tRNA^{Lys} primer and genomic RNA template in the reverse transcription complex. In vitro studies of recombinant RT with either the W401L or W401A mutation also demonstrated a complete inhibition of RNA-dependent DNA polymerase activity using the same synthetic template/primer used for our RT assays (51) and also using a template/primer based on the HIV-1 sequence (53). Therefore, one explanation for the difference in RT activity in infected cells compared to that in vitro may be due to the stabilizing presence of other viral or host cell factors that modulate RT activity in the reverse transcription complex (17, 19, 54, 55, 63). Another possibility for the difference in RT activity of W401 mutants in cell-free assays compared to intracellular reverse transcription can be ascribed to the dimerization constant of the RT. The effective concentration of RT in the confines of the reverse transcription complex is likely higher than that in cell-free assays. Hence, the proportions of dimers and monomers in the reverse transcription complex would be higher, leading to a less dramatic defect than what we observed in the cell-free assays.

Our study demonstrates a clear correlation between RT dimerization-inhibiting mutations located near the RT dimer interface and defects in RT maturation and function. The defect in RT function was observed in the absence of detect-

able effects on Gag-Pol stability or Gag-Pol incorporation into the virion. Our studies suggest that the most likely precursor of the mature RT heterodimer in HIV-1-infected cells is the p66 homodimer, although further studies are needed to prove this assertion. Since the stability of the p66 homodimer is orders of magnitude lower than that of the RT heterodimer, the former represents a more attractive target for destabilization by small-molecule inhibitors of HIV-1 RT.

ACKNOWLEDGMENTS

G.T. was supported by NHMRC career development award 235102 and NHMRC project grant 235030. J.W. was supported by the Australian Postgraduate Award, Monash University.

We thank Dag Helland for the supply of RT and IN antibodies, Andy Poumbourios for the purification of p24 antibodies, and the NIH AIDS Research and Reference Reagent Program, Division of AIDS, NIAID, NIH, for the supply of indinavir, the TZM-bl cell line, and the p24 hybridoma (183-H12-5C). We thank Margaret Hellard for assistance with the statistical analyses performed for this study.

REFERENCES

1. **Adachi, A., H. E. Gendelman, S. Koenig, T. Folks, R. Willey, A. Rabson, and M. A. Martin.** 1986. Production of acquired immunodeficiency syndrome-associated retrovirus in human and nonhuman cells transfected with an infectious molecular clone. J. Virol. **59:**284–291.
2. **Amacker, M., and U. Hubscher.** 1998. Chimeric HIV-1 and feline immunodeficiency virus reverse transcriptases: critical role of the p51 subunit in the structural integrity of heterodimeric lentiviral DNA polymerases. J. Mol. Biol. **278:**757–765.
3. **Baillon, J. G., N. T. Nashed, A. Kumar, S. H. Wilson, and D. M. Jerina.** 1991. A leucine zipper-like motif may mediate HIV reverse transcriptase subunit binding. New Biol. **3:**1015–1019.
4. **Becerra, S. P., A. Kumar, M. S. Lewis, S. G. Widen, J. Abbotts, E. M. Karawya, S. H. Hughes, J. Shiloach, and S. H. Wilson.** 1991. Protein-protein interactions of HIV-1 reverse transcriptase: implication of central and C-terminal regions in subunit binding. Biochemistry **30:**11707–11719.
5. **Bhattacharyya, G. K., and R. A. Johnson.** 1997. Statistical concepts and methods. John Wiley and Sons, New York, N.Y.
6. **Buxton, P., G. Tachedjian, and J. Mak.** 2005. Analysis of the contribution of reverse transcriptase and integrase proteins to retroviral RNA dimer conformation. J. Virol. **79:**6338–6348.
7. **Chesebro, B., K. Wehrly, J. Nishio, and S. Perryman.** 1992. Macrophage-tropic human immunodeficiency virus isolates from different patients exhibit unusual V3 envelope sequence homogeneity in comparison with T-cell-tropic isolates: definition of critical amino acids involved in cell tropism. J. Virol. **66:**6547–6554.
8. **Derdeyn, C. A., J. M. Decker, J. N. Sfakianos, X. Wu, W. A. O'Brien, L. Ratner, J. C. Kappes, G. M. Shaw, and E. Hunter.** 2000. Sensitivity of human immunodeficiency virus type 1 to the fusion inhibitor T-20 is modulated by coreceptor specificity defined by the V3 loop of gp120. J. Virol. **74:**8358–8367.
9. **di Marzo Veronese, F., T. D. Copeland, A. L. DeVico, R. Rahman, S. Oroszlan, R. C. Gallo, and M. G. Sarngadharan.** 1986. Characterization of highly immunogenic p66/p51 as the reverse transcriptase of HTLV-III/LAV. Science **231:**1289–1291.
10. **Divita, G., T. Restle, and R. S. Goody.** 1993. Characterization of the dimerization process of HIV-1 reverse transcriptase heterodimer using intrinsic protein fluorescence. FEBS Lett. **324:**153–158.
11. **Divita, G., K. Rittinger, T. Restle, U. Immendorfer, and R. S. Goody.** 1995. Conformational stability of dimeric HIV-1 and HIV-2 reverse transcriptases. Biochemistry **34:**16337–16346.
12. **Fisher, A. G., E. Collalti, L. Ratner, R. C. Gallo, and F. Wong-Staal.** 1985. A molecular clone of HTLV-III with biological activity. Nature **316:**262–265.
13. **Folks, T. M., K. A. Clouse, J. Justement, A. Rabson, E. Duh, J. H. Kehrl, and A. S. Fauci.** 1989. Tumor necrosis factor alpha induces expression of human immunodeficiency virus in a chronically infected T-cell clone. Proc. Natl. Acad. Sci. USA **86:**2365–2368.
14. **Ghosh, M., P. S. Jacques, D. W. Rodgers, M. Ottman, J. L. Darlix, and S. F. Le Grice.** 1996. Alterations to the primer grip of p66 HIV-1 reverse transcriptase and their consequences for template-primer utilization. Biochemistry **35:**8553–8562.
15. **Gorelick, R. J., and L. E. Henderson.** 1994. Human retroviruses and AIDS: analyses (part III). The Los Alamos National Laboratory, Los Alamos, N.Mex.
16. **Harada, S., Y. Koyanagi, and N. Yamamoto.** 1985. Infection of HTLV-III/LAV in HTLV-I-carrying cells MT-2 and MT-4 and application in a plaque assay. Science **229:**563–566.
17. **Harrich, D., and B. Hooker.** 2002. Mechanistic aspects of HIV-1 reverse transcription initiation. Rev. Med. Virol. **12:**31–45.
18. **Hawkes, R.** 1979. General principles underlying laboratory diagnosis in viral infections, p. 34–35. *In* Diagnostic procedures for viral, rickettsial and chlamydial infection, 5th ed. American Public Health Association, Washington, D.C.
19. **Hehl, E. A., P. Joshi, G. V. Kalpana, and V. R. Prasad.** 2004. Interaction between human immunodeficiency virus type 1 reverse transcriptase and integrase proteins. J. Virol. **78:**5056–5067.
20. **Henderson, L. E., M. A. Bowers, R. C. Sowder II, S. A. Serabyn, D. G. Johnson, J. W. Bess, Jr., L. O. Arthur, D. K. Bryant, and C. Fenselau.** 1992. Gag proteins of the highly replicative MN strain of human immunodeficiency virus type 1: posttranslational modifications, proteolytic processing, and complete amino acid sequences. J. Virol. **66:**1856–1865.
21. **Hill, M., G. Tachedjian, and J. Mak.** 2005. The packaging and maturation of the HIV-1 Pol proteins. Curr. HIV Res. **3:**73–85.
22. **Hill, M. K., M. Shehu-Xhilaga, S. M. Crowe, and J. Mak.** 2002. Proline residues within spacer peptide p1 are important for human immunodeficiency virus type 1 infectivity, protein processing, and genomic RNA dimer stability. J. Virol. **76:**11245–11253.
23. **Hostomsky, Z., Z. Hostomska, T. B. Fu, and J. Taylor.** 1992. Reverse transcriptase of human immunodeficiency virus type 1: functionality of subunits of the heterodimer in DNA synthesis. J. Virol. **66:**3179–3182.
24. **Jacobo-Molina, A., J. Ding, R. G. Nanni, A. D. Clark, Jr., X. Lu, C. Tantillo, R. L. Williams, G. Kamer, A. L. Ferris, P. Clark, et al.** 1993. Crystal structure of human immunodeficiency virus type 1 reverse transcriptase complexed with double-stranded DNA at 3.0 A resolution shows bent DNA. Proc. Natl. Acad. Sci. USA **90:**6320–6324.
25. **Jacques, P. S., B. M. Wohrl, K. J. Howard, and S. F. Le Grice.** 1994. Modulation of HIV-1 reverse transcriptase function in "selectively deleted" p66/p51 heterodimers. J. Biol. Chem. **269:**1388–1393.
26. **Jacques, P. S., B. M. Wohrl, M. Ottmann, J. L. Darlix, and S. F. Le Grice.** 1994. Mutating the "primer grip" of p66 HIV-1 reverse transcriptase implicates tryptophan-229 in template-primer utilization. J. Biol. Chem. **269:**26472–26478.
27. **Kaplan, A. H., M. Manchester, and R. Swanstrom.** 1994. The activity of the protease of human immunodeficiency virus type 1 is initiated at the membrane of infected cells before the release of viral proteins and is required for release to occur with maximum efficiency. J. Virol. **68:**6782–6786.
28. **Klein, J. R., and B. D. Jones.** 2001. *Salmonella* pathogenicity island 2-encoded proteins SseC and SseD are essential for virulence and are substrates of the type III secretion system. Infect. Immun. **69:**737–743.
29. **Kohlstaedt, L. A., J. Wang, J. M. Friedman, P. A. Rice, and T. A. Steitz.** 1992. Crystal structure at 3.5 A resolution of HIV-1 reverse transcriptase complexed with an inhibitor. Science **256:**1783–1790.
30. **Lee, T. H., F. J. Sunzeri, L. H. Tobler, B. G. Williams, and M. P. Busch.** 1991. Quantitative assessment of HIV-1 DNA load by coamplification of HIV-1 gag and HLA-DQ-alpha genes. AIDS **5:**683–691.
31. **Le Grice, S. F., C. E. Cameron, and S. J. Benkovic.** 1995. Purification and characterization of human immunodeficiency virus type 1 reverse transcriptase. Methods Enzymol. **262:**130–144.
32. **Le Grice, S. F., T. Naas, B. Wohlgensinger, and O. Schatz.** 1991. Subunit-selective mutagenesis indicates minimal polymerase activity in heterodimer-associated p51 HIV-1 reverse transcriptase. EMBO J. **10:**3905–3911.
33. **Lindhofer, H., K. von der Helm, and H. Nitschko.** 1995. In vivo processing of Pr160gag-pol from human immunodeficiency virus type 1 (HIV) in acutely infected, cultured human T-lymphocytes. Virology **214:**624–627.
34. **Mak, J., A. Khorchid, Q. Cao, Y. Huang, I. Lowy, M. A. Parniak, V. R. Prasad, M. A. Wainberg, and L. Kleiman.** 1997. Effects of mutations in Pr160gag-pol upon tRNA(Lys3) and Pr160gag-pol incorporation into HIV-1. J. Mol. Biol. **265:**419–431.
35. **Mulky, A., S. G. Sarafianos, E. Arnold, X. Wu, and J. C. Kappes.** 2004. Subunit-specific analysis of the human immunodeficiency virus type 1 reverse transcriptase in vivo. J. Virol. **78:**7089–7096.
36. **Nilsen, B. M., I. R. Haugan, K. Berg, L. Olsen, P. O. Brown, and D. E. Helland.** 1996. Monoclonal antibodies against human immunodeficiency virus type 1 integrase: epitope mapping and differential effects on integrase activities in vitro. J. Virol. **70:**1580–1587.
37. **Patel, P. H., A. Jacobo-Molina, J. Ding, C. Tantillo, A. D. Clark, Jr., R. Raag, R. G. Nanni, S. H. Hughes, and E. Arnold.** 1995. Insights into DNA polymerization mechanisms from structure and function analysis of HIV-1 reverse transcriptase. Biochemistry **34:**5351–5363.
38. **Pear, W. S., G. P. Nolan, M. L. Scott, and D. Baltimore.** 1993. Production of high-titer helper-free retroviruses by transient transfection. Proc. Natl. Acad. Sci. USA **90:**8392–8396.
39. **Pettit, S. C., L. E. Everitt, S. Choudhury, B. M. Dunn, and A. H. Kaplan.** 2004. Initial cleavage of the human immunodeficiency virus type 1 GagPol precursor by its activated protease occurs by an intramolecular mechanism. J. Virol. **78:**8477–8485.
40. **Pettit, S. C., S. Gulnik, L. Everitt, and A. H. Kaplan.** 2003. The dimer interfaces of protease and extra-protease domains influence the activation of protease and the specificity of GagPol cleavage. J. Virol. **77:**366–374.

41. **Restle, T., B. Muller, and R. S. Goody.** 1990. Dimerization of human immunodeficiency virus type 1 reverse transcriptase. A target for chemotherapeutic intervention. J. Biol. Chem. **265:**8986–8988.
42. **Richardson, B. A., and J. Overbaugh.** 2005. Basic statistical considerations in virological experiments. J. Virol. **79:**669–676.
43. **Shehu-Xhilaga, M., S. Ablan, D. G. Demirov, C. Chen, R. C. Montelaro, and E. O. Freed.** 2004. Late domain-dependent inhibition of equine infectious anemia virus budding. J. Virol. **78:**724–732.
44. **Shin, C. G., B. Taddeo, W. A. Haseltine, and C. M. Farnet.** 1994. Genetic analysis of the human immunodeficiency virus type 1 integrase protein. J. Virol. **68:**1633–1642.
45. **Sluis-Cremer, N., D. Arion, M. E. Abram, and M. A. Parniak.** 2004. Proteolytic processing of an HIV-1 Pol polyprotein precursor: insights into the mechanism of reverse transcriptase p66/p51 heterodimer formation. Int. J. Biochem. Cell Biol. **36:**1836–1847.
46. **Sluis-Cremer, N., D. Arion, and M. A. Parniak.** 2002. Destabilization of the HIV-1 reverse transcriptase dimer upon interaction with *N*-acyl hydrazone inhibitors. Mol. Pharmacol. **62:**398–405.
47. **Sluis-Cremer, N., G. I. Dmitrienko, J. Balzarini, M. J. Camarasa, and M. A. Parniak.** 2000. Human immunodeficiency virus type 1 reverse transcriptase dimer destabilization by 1-[spiro[4"-amino-2",2"-dioxo-1",-2"-oxathiole-5",3′-[2′,5′-*bis*-*O*-(*tert*-butyldimethylsilyl)-beta-D-ribofuranosyl]]]-3-ethylthymine. Biochemistry **39:**1427–1433.
48. **Sluis-Cremer, N., and G. Tachedjian.** 2002. Modulation of the oligomeric structures of HIV-1 retroviral enzymes by synthetic peptides and small molecules. Eur. J. Biochem. **269:**5103–5111.
49. **Sonza, S., A. Maerz, N. Deacon, J. Meanger, J. Mills, and S. Crowe.** 1996. Human immunodeficiency virus type 1 replication is blocked prior to reverse transcription and integration in freshly isolated peripheral blood monocytes. J. Virol. **70:**3863–3869.
50. **Szilvay, A. M., S. Nornes, I. R. Haugan, L. Olsen, V. R. Prasad, C. Endresen, S. P. Goff, and D. E. Helland.** 1992. Epitope mapping of HIV-1 reverse transcriptase with monoclonal antibodies that inhibit polymerase and RNase H activities. J. Acquir. Immune Defic. Syndr. **5:**647–657.
51. **Tachedjian, G., H. E. Aronson, M. de los Santos, J. Seehra, J. M. McCoy, and S. P. Goff.** 2003. Role of residues in the tryptophan repeat motif for HIV-1 reverse transcriptase dimerization. J. Mol. Biol. **326:**381–396.
52. **Tachedjian, G., H. E. Aronson, and S. P. Goff.** 2000. Analysis of mutations and suppressors affecting interactions between the subunits of the HIV type 1 reverse transcriptase. Proc. Natl. Acad. Sci. USA **97:**6334–6339.
53. **Tachedjian, G., J. Radzio, and N. Sluis-Cremer.** 2005. Relationship between enzyme activity and dimeric structure of recombinant HIV-1 reverse transcriptase. Proteins **60:**5–13.
54. **Tasara, T., M. O. Hottiger, and U. Hubscher.** 2001. Functional genomics in HIV-1 virus replication: protein-protein interactions as a basis for recruiting the host cell machinery for viral propagation. Biol. Chem. **382:**993–999.
55. **Tasara, T., G. Maga, M. O. Hottiger, and U. Hubscher.** 2001. HIV-1 reverse transcriptase and integrase enzymes physically interact and inhibit each other. FEBS Lett. **507:**39–44.
56. **Telesnitsky, A., and S. P. Goff.** 1993. Two defective forms of reverse transcriptase can complement to restore retroviral infectivity. EMBO J. **12:**4433–4438.
57. **Vacca, J. P., B. D. Dorsey, W. A. Schleif, R. B. Levin, S. L. McDaniel, P. L. Darke, J. Zugay, J. C. Quintero, O. M. Blahy, E. Roth, et al.** 1994. L-735,524: an orally bioavailable human immunodeficiency virus type 1 protease inhibitor. Proc. Natl. Acad. Sci. USA **91:**4096–4100.
58. **Vogt, V. M.** 1996. Morphogenesis and maturation of retroviruses, vol. 214. Springer-Verlag, Berlin, Germany.
59. **Wang, J., S. J. Smerdon, J. Jager, L. A. Kohlstaedt, P. A. Rice, J. M. Friedman, and T. A. Steitz.** 1994. Structural basis of asymmetry in the human immunodeficiency virus type 1 reverse transcriptase heterodimer. Proc. Natl. Acad. Sci. USA **91:**7242–7246.
60. **Wei, X., J. M. Decker, H. Liu, Z. Zhang, R. B. Arani, J. M. Kilby, M. S. Saag, X. Wu, G. M. Shaw, and J. C. Kappes.** 2002. Emergence of resistant human immunodeficiency virus type 1 in patients receiving fusion inhibitor (T-20) monotherapy. Antimicrob. Agents Chemother. **46:**1896–1905.
61. **Wiegers, K., G. Rutter, H. Kottler, U. Tessmer, H. Hohenberg, and H. G. Krausslich.** 1998. Sequential steps in human immunodeficiency virus particle maturation revealed by alterations of individual Gag polyprotein cleavage sites. J. Virol. **72:**2846–2854.
62. **Wohrl, B. M., R. Krebs, S. H. Thrall, S. F. Le Grice, A. J. Scheidig, and R. S. Goody.** 1997. Kinetic analysis of four HIV-1 reverse transcriptase enzymes mutated in the primer grip region of p66. Implications for DNA synthesis and dimerization. J. Biol. Chem. **272:**17581–17587.
63. **Wu, X., H. Liu, H. Xiao, J. A. Conway, E. Hehl, G. V. Kalpana, V. Prasad, and J. C. Kappes.** 1999. Human immunodeficiency virus type 1 integrase protein promotes reverse transcription through specific interactions with the nucleoprotein reverse transcription complex. J. Virol. **73:**2126–2135.
64. **Wu, X., H. Liu, H. Xiao, J. A. Conway, E. Hunter, and J. C. Kappes.** 1997. Functional RT and IN incorporated into HIV-1 particles independently of the Gag/Pol precursor protein. EMBO J. **16:**5113–5122.
65. **Yu, Q., M. Ottmann, C. Pechoux, S. Le Grice, and J. L. Darlix.** 1998. Mutations in the primer grip of human immunodeficiency virus type 1 reverse transcriptase impair proviral DNA synthesis and virion maturation. J. Virol. **72:**7676–7680.
66. **Zack, J. A., S. J. Arrigo, S. R. Weitsman, A. S. Go, A. Haislip, and I. S. Chen.** 1990. HIV-1 entry into quiescent primary lymphocytes: molecular analysis reveals a labile, latent viral structure. Cell **61:**213–222.